Design, Construction and Test of a Small Bitter Magnet usable for a Hybrid Magnet

Design, Construction and Test of a Small Bitter Magnet usable for a Hybrid Magnet*

Yasuaki Nakagawa, Shigeto Miura, Akira Hoshi, Minoru Kudo,
Kuniaki Sai and Yoshimi Ishikawa
The Research Institute for Iron, Steel and Other Metals

(Received June 10, 1981)

Synopsis

A hybrid magnet is a combined system of an outer superconducting magnet and an inner high-power water-cooled magnet, generating continuous high magnetic fields. A small Bitter coil to be used for the latter magnet has been designed, constructed and tested up to the DC electric power of 3 MW and the deionized-water flow rate of 130 m^3/h. According to expectations, the field produced in a clear bore of 32 mm diameter has reached 12.4 T without an excessive temperature rise of the coil.

I. Introduction

Continuous high magnetic fields have been generated by either high-power water-cooled magnets or superconducting magnets. The former facilities were established in our institute in 1958, where a 3.5-MW DC electric source and a 60-m^3/h deionized-water cooling system were installed[1,2]. The fields up to 10 T have been obtained by the so-called Bitter coils[3] and used for various solid-state experiments. Since 1960's, developments in high-field superconductors enable us to generate 10 T fields much more easily. In order to produce higher fields, however, it is advantageous to combine an outer superconducting coil and an inner high-power water-cooled coil, as was first suggested by Wood and Montgomery[4]. Such a system is usually called a hybrid magnet[5].

The hybrid magnet project is also being pushed forward at our institute. The Bitter coil with a smaller outer diameter is necessary for this purpose. It has been planned, for example, that the outer superconducting magnet has a room-temperature bore of 220 mm, giving

---

* The 1743th report of the Research Institute for Iron, Steel and Other Metals.

a field of 8 T, and the inner Bitter coil has an outer diameter of 182 mm and inner diameter of 37 mm, giving a field of 13 T by the use of 3.5-MW power; the total field in a clear bore of 32 mm will exceed 20 T. The present report describes the design, construction and test of the new Bitter coil. The test could be made up to 3-MW power and 130-m^3/h flow rate, since the capacity of our deionized-water cooling system had recently been doubly augmented.

II. Design

The Bitter coil consists of alternate disks of conductor and insulator with a radial slit, which are partly overlapped to form a spiral conducting path. As shown in Fig. 1, each disk has small cooling holes with radius h which are distributed on concentric circles with radii a_i (i = 1, 2, -----, n). The inner and outer radii of the disk are denoted as a_0 and a_{n+1}, respectively. There are m holes on each circle, the total number being m × n. It is considered that the Bitter disk is split into concentric annular segments, the inner and outer radii of the i-th segment being a_{i-1} and a_i, respectively. The density of circular electric current would be inversely proportional to

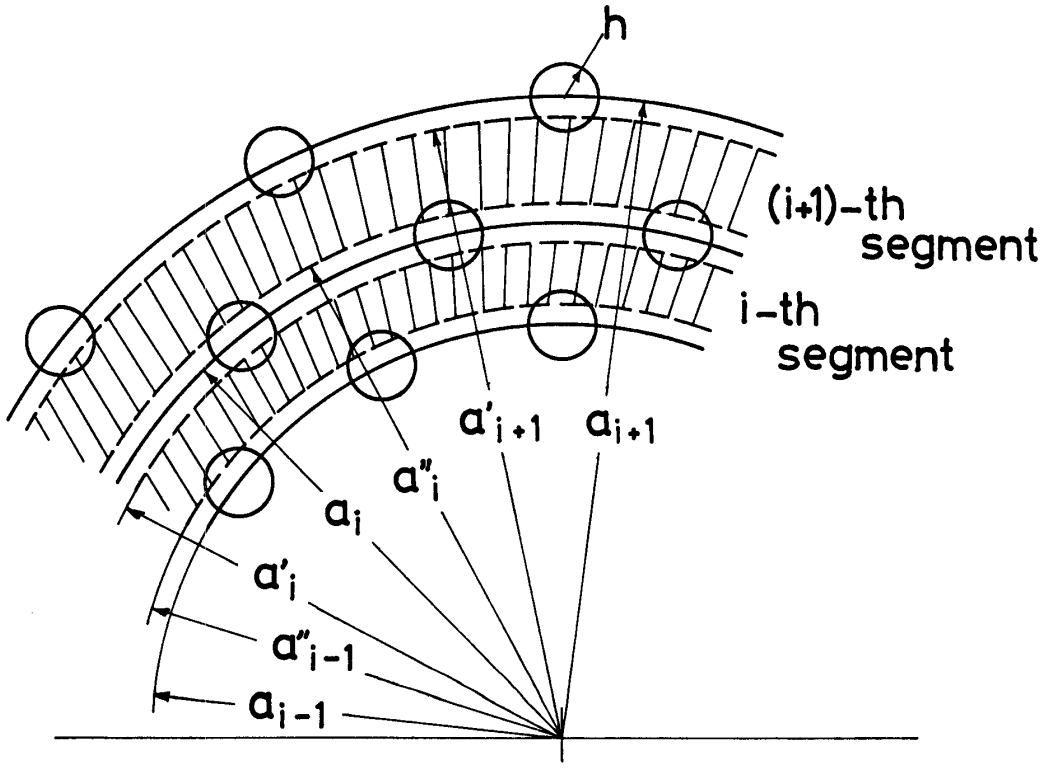

Fig. 1. Distribution of cooling holes in a Bitter disk.

the distance from the central axis if there were no cooling holes. The effect of the cooling holes are treated as follows: the electric resistance of the i-th segment is equivalent to that of a fictitious annulus with the inner radius a''_{i-1} and the outer radius a'_i, as indicated by a hatched region in Fig. 1. These values are given by Clement's empirical equations[6]:

$$\ln a'_i = \ln a_i + [1 - \exp(-\alpha m h/\pi a_i)] \ln(1 - h/a_i) ,$$
$$\ln a''_i = \ln a_i + [1 - \exp(-\alpha m h/\pi a_i)] \ln(1 + h/a_i) , \tag{1}$$

where α is an adjustable constant. According to Clement, the best value for α is 1.9. The electric current through the i-th segment is

$$I_i = \int_{a''_{i-1}}^{a'_i} \frac{V_0 t}{2\pi\rho r} dr = \frac{V_0 t}{2\pi\rho} \ln \frac{a'_i}{a''_{i-1}} , \tag{2}$$

where t is the thickness of the disk, ρ the resistivity and V_0 the electric potential difference of a round path.

The most efficient cooling is realized when the temperature rise in the coil is uniform, so the Joule heating and the water cooling must be balanced in each segment. The cooling surface for each segment is provided by semi-holes on the inner and outer circles, the surface area being given by $S = 2\pi htm$. Since S is the same for all segments, I_i must be the same for i = 2, 3, -----, n. Actually the values of a_i are determined so as to satisfy the condition that a'_i/a''_{i-1} is nearly constant. The innermost (i = 1) and outermost (i = n + 1) segments have to be treated otherwise, since there are no cooling holes on the inner circle of the former nor the outer circle of the latter. It is reasonable to assume that $a''_0 = a_0$ and $a'_{n+1} = a_{n+1}$, contrary to eq. (1). The cooling surface can also be provided by the inner and outer boundaries of the disk, I_1 and I_{n+1} being determined to realize the same temperature rise. In the present design, only the inner boundary of the disk, with the surface area $S' = 2\pi a_0 t$, is water-cooled.

Figure 2 shows a photograph of the Bitter disk, the cooling-hole pattern being determined under the conditions that n = 15, m = 36, h = 1.1 (mm), a_0 = 18.5 (mm) and a_{n+1} = 91 (mm). There are 12 larger holes for bolts to support a stack of the conductor and insulator disks. The conductor disk has a sectorial opening of 10°. The

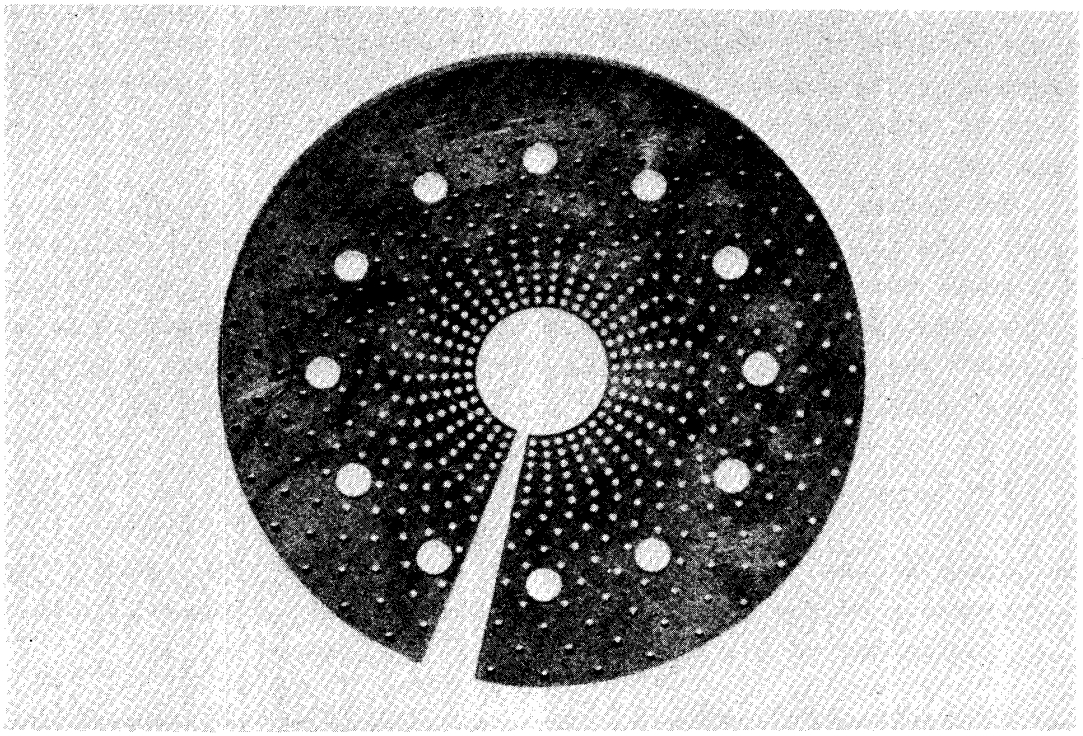

Fig. 2. Bitter disk of 182-mm outer diameter.

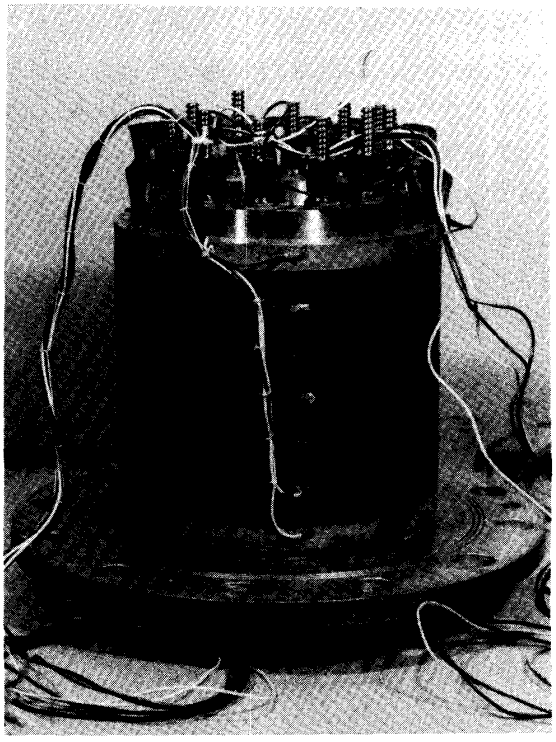

Fig. 3. Bitter coil with potential leads.

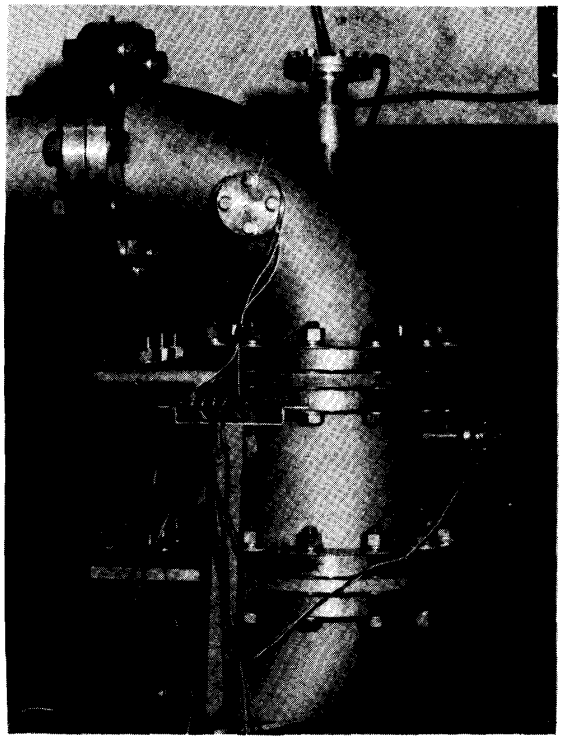

Fig. 4. Bitter magnet with water pipes.

adjacent conductor disks are rotated by 30°, and the 20°-sector portions are directly contacted without the insulator disk. The disturbance of the current density due to the larger holes is ignored although it is not negligibly small. The contact resistance is also neglected.

The Bitter coil consisting of N conductor disks has (11/12)N turns. Its electric resistance is (8/9)NR, where R is the resistance of a sheet of the disk without opening and overlapping. A small correction for the resistance at upper and lower ends of the coil is also ignored. The current through the coil is (9/8)V/NR, where V is the voltage applied to the coil. It is derived from eq.(1) that

$$I = \frac{9}{8}\frac{V}{N}\frac{t}{2\pi\rho}\sum_{i=1}^{n+1}\ln\frac{a'_i}{a''_{i-1}} \qquad (3)$$

The height of the coil is approximated by $\ell = N(t + t')$, where t' is the thickness of the insulator disk. The magnetic field (flux density) B_0 at the center of the coil is also derived from eq.(1) as

$$B_0 = \frac{33}{32}\cdot\frac{\mu_0 Vt}{2\pi\rho\ell}\sum_{i=1}^{n+1}\left[\ln\frac{a'_i}{a''_{i-1}}\Bigg/\sqrt{1+\left(\frac{2\bar{a}_i}{\ell}\right)^2}\right], \qquad (4)$$

with $\bar{a}_i = (a_i + a_{i-1})/2$ and $\mu_0 = 4\pi \times 10^{-7}$ in SI units.

It is chosen here that N = 200, t = 0.6 (mm) and t' = 0.1 (mm). The conductor used is pure copper. Since the temperature may reach around 80 °C, ρ is assumed to be 2.1×10^{-8} Ωm. For the coil with the disk shown in Fig. 2, it is calculated with eq.(3) that I = 9.22 (kA) at V = 300 (V), the total power amounting to W = 2.77 (MW). It is also evaluated that ℓ = 140 (mm) and B_0 = 12.4 (T), and then B_0/I = 1.34 (T/kA). Since the total area of the cooling surface in the coil, $A = N(nS + S')$, is calculated to be 0.46 m^2, the rate of heat transfer between conductor and water is expected as $W/A = 6.0$ (W/mm^2).

III. Construction

Conductor disks were made of 1/4 H-copper plates of 0.6-mm thickness, and insulator disks of glass-fiber-enforced polyimide sheets ('Imidalloy' of Toshiba Chemical Products Co.) of 0.1-mm thickness. Inner and outer boundaries and 12 holes of 10-mm diameter were firstly punched with a 30-ton press, then 528 holes of 2.2-mm diameter were punched in 12 instalments by using the 10-mm hole as a guide, and finally a narrow sectorial opening was cut off. The surface of copper disks was slightly polished with emery paper and cleaned with

organic solvent. Neither annealing nor silver plating was applied to the disks.

Two-hundred sheets of conductor and insulator disks were stacked alternately, as already mentioned. Upper and lower ends of the coil were heavy brass electrodes with similar holes for cooling water and supporting bolts. Several sheets of dummy conductor disks were inserted between the electrods and the effective conductor disks in order to convert vertical current into spiral current smoothly. The supporting bolts were made of stainless steel covered with glass-fiber-enforced epoxy tube of 1-mm wall thickness. The stack of the disks and electrodes were tightly fastened by nuts with insulating washers, as shown in Fig. 3. There can be seen several potential leads to measure the electric resistance, from which the average temperatures of the conductors are estimated. Thermocouples were also set for measuring water temperatures near the conductor.

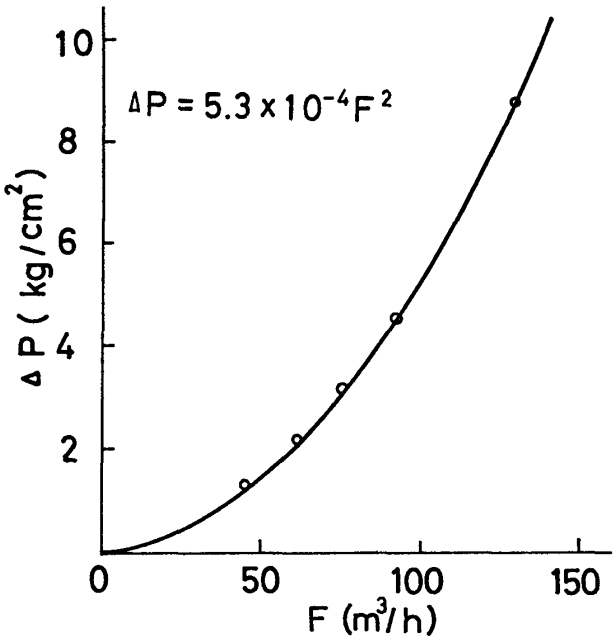

Fig. 5. Pressure difference ΔP vs flow rate F of the Bitter coil.

The Bitter coil was placed inside a stainless-steel case with inlet and outlet pipes for deionized water. Its external appearence is shown in Fig. 4. Heavy electric leads were connected with the 3.5-MW electric source. A stainless-steel tube of 34-mm outer diameter and 32-mm inner diameter was inserted along the central axis of the coil, in which a Hall probe for measuring the magnetic field was placed. An insulator sheet was wound outside the tube, leaving an annular spacing of about 1 mm from the inner boundary of the coil. The water-flow velocity in this spacing is estimated to be not so different from that in the cooling holes. The water flow along the outer boundary of the coil was almost inhibited.

IV. Test

Figure 5 shows the pressure difference of flowing water between the inlet and outlet pipes, ΔP in kg/cm^2, plotted as a function of the

flow rate, F in m^3/h, exhibiting a parabolic relation. The pressure difference for turbulent flow in a tube with entrance and exit losses is given by a hydraulic equation[7],

$$\Delta P = \left(\frac{3}{2} + f\frac{\ell'}{d}\right)\frac{1}{2}\mu v^2 \quad , \tag{5}$$

in SI units, where v is the flow velocity, μ the density, d the diameter and ℓ' the length of the tube. The friction factor f depends on relative roughness ε (the deviation in diameter over the tube diameter) and Reynolds number $Re = \mu vd/\eta$ (η: viscosity)[8]; if the tube is smooth ($\varepsilon = 0$), then $f = 0.184\,Re^{-0.2}$; if Re is sufficiently large, then $f = 0.24\,\varepsilon^{0.4}$. For the present Bitter coil, $d = 2h = 0.22$ (cm), $\ell' = \ell + 4 = 18$ (cm), and v (m/s) = 0.13 F (m^3/h) since the cooling-channel cross-section is 21 cm^2. Comparing eq.(5) with the experimental result, we obtain f = 0.06. Since $\mu = 10^3$ (kg/m^3), $\eta = 7 \sim 3 \times 10^{-4}$ (kg/m/s) at 30 ∿ 100 °C, and $F \geq 46$ (m^3/h), so $Re \geq 1.8 \times 10^4$. It is thus derived, that $\varepsilon = 0.03$, as expected from the rough surface of cooling channel through conductor and insulater disks.

The relation between voltage and current is shown in Fig. 6. The curves are concave upwards and depend on the flow rate of water, resulting from an appreciable temperature dependence of the conductor resistance. The current amounted to 9.10 kA at the voltage of 300 V, in good agreement with that estimated in section II, suggesting that the contact resistance between the disks was sufficiently small.

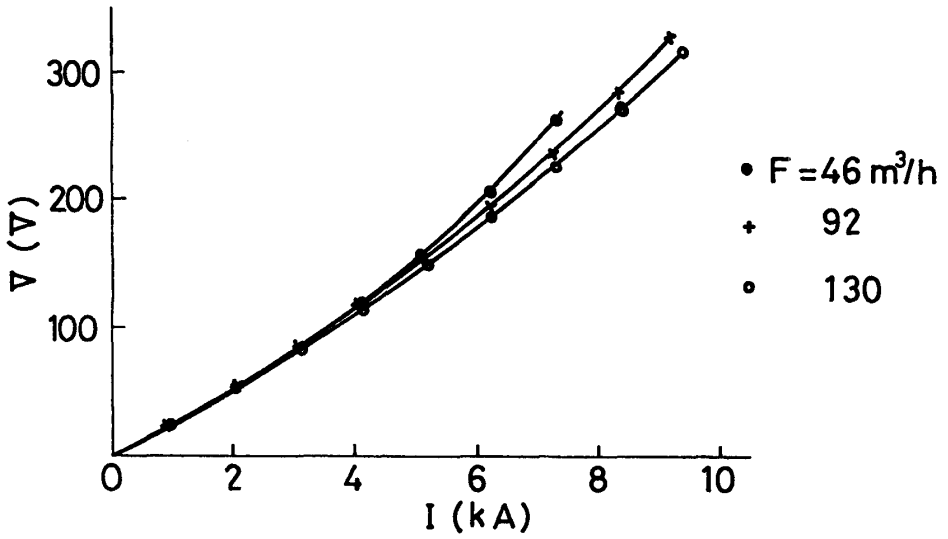

Fig. 6. Current I vs voltage V of the Bitter coil in the case of water-flow rate F.

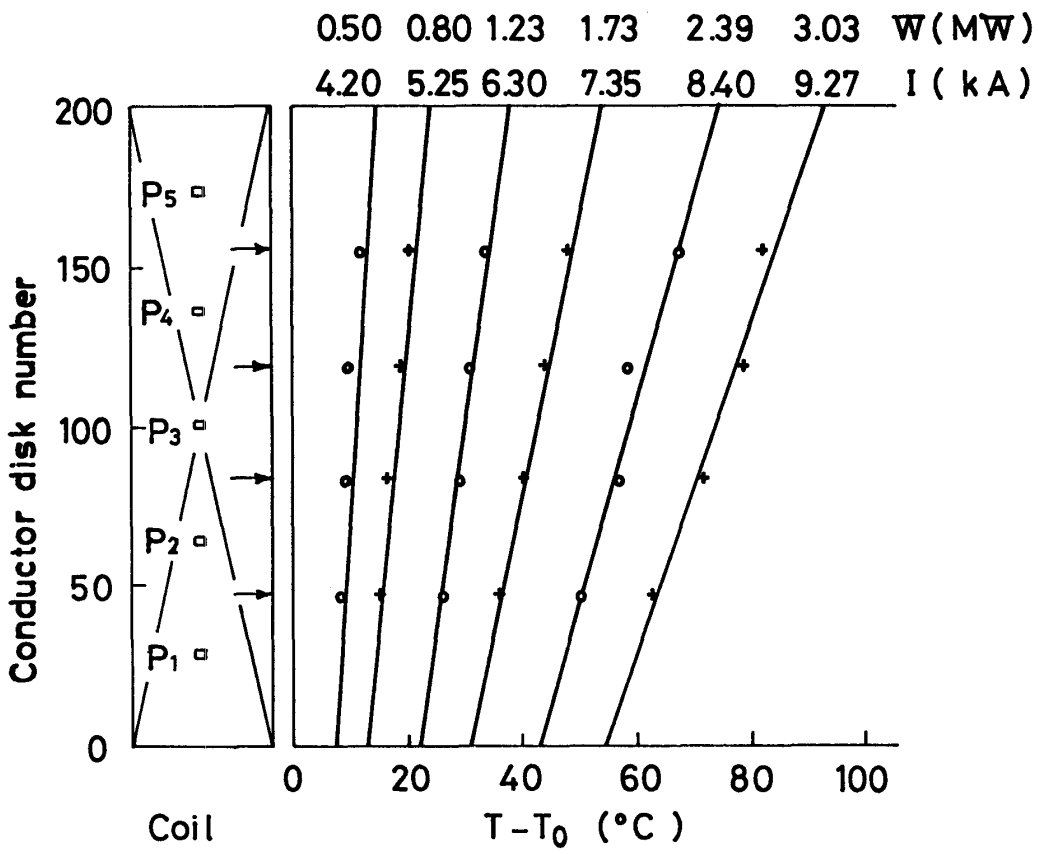

Fig. 7. Temperature distribution in the coil with current I, power W and water flow rate of 92 m^3/h, estimated from the resistivity change between potential leads P_i. Arrows indicate mid points of the adjacent leads.

The temperature of flowing water in the coil shows a linear increase along the coil axis. In a steady state the temperature difference between outlet and inlet, ΔT in °C, is simply derived from the heat capacity of water as

$$\Delta T = 860\ W/F \quad , \tag{6}$$

where W is the total power in MW and F the flow rate in m^3/h. This relation could easily be verified by the present test because the system reached a steady state fairly quickly. The temperature difference between flowing water and surrounding conductor, δT, is nearly constant everywhere and related to the heat-transfer coefficient, H, as

$$H\,\delta T = W/A \quad , \tag{7}$$

where A is the total area of the interface between water and conductor. As already mentioned in section II , it was expected that W/A = 6.5 (W/mm^2) at W = 3.0 (MW). In order to obtain the value of H in the

present test, the temperature of the conductor was estimated from the electric resistance measured by the use of potential leads.

As illustrated in Fig. 7, the potential leads were placed at 29th, 65th, 101st, 137th and 173rd disks. The potential difference, ϕ, between adjacent leads were measured as a function of the current, I, through the coil. Since ϕ/I is proportional to the resistance, the temperature, T, is given by

$$T - T_0 = \frac{1}{\alpha} \frac{(\phi/I) - (\phi/I)_0}{(\phi/I)_0} \quad , \tag{8}$$

where T_0 is the initial temperature, α is the temperature coefficient of the resistivity, and $(\phi/I)_0$ is the limiting value of (ϕ/I) as the current tends to zero. The temperature thus obtained is an average temperature of the conductor in between the adjacent potential leads. For the leads of 29th and 65th disks, for example, T corresponds to the temperature of 47th disk. The temperature coefficient of the resistivity of copper depends slightly on the initial temperature. Since the resistivity at T °C is well expressed as $\rho = (1.60 + 0.006\,T) \times 10^{-8}$ (Ωm), it is obtained that $\alpha = 3.7 \times 10^{-3}$ ($°C^{-1}$) at $T_0 = 6$ (°C).

Measurements of the potential difference were made for various flow rates of water. As an example, the results for F = 92 (m^3/h) and $T_0 = 6$ (°C) are shown in Fig. 7. The larger the current and the power, the steeper becomes the temperature gradient in the coil. The temperatures at upper and lower ends of the coil, T_u and T_ℓ respectively, were obtained by extrapolation. These are plotted against the power in Fig. 8, together with the temperature rise of flowing water, ΔT of eq. (6), which should be equal to $T_u - T_\ell$ although the discrepancy is not so small. The temperature difference between water and conductor, δT, may be given by $T_\ell - T_0$. Strictly speaking, however,

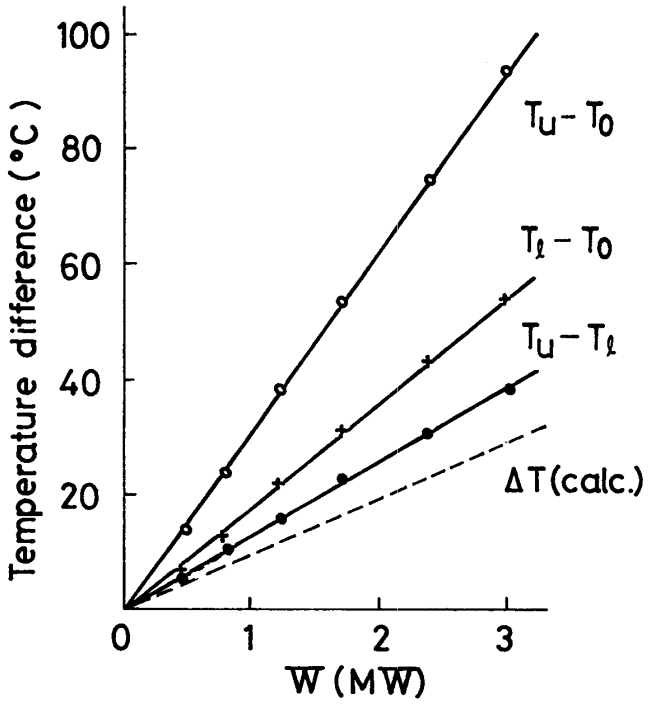

Fig. 8. Temperatures of upper (T_u) and lower (T_ℓ) ends of the coil with power W. ΔT is the temperature rise of 92-m^3/h water.

the average temperature of the conductor is different from the cooling-surface temperature because the thermal conductivity of cooper is not infinite.

The temperature distribution in the conductor is roughly estimated as follows: if an annular plate, with the outer radius b, inner radius h and thickness t, is uniformly heated by the power P and cooled by the inner boundary, the temperature difference between the outer and inner boundaries in a steady state is

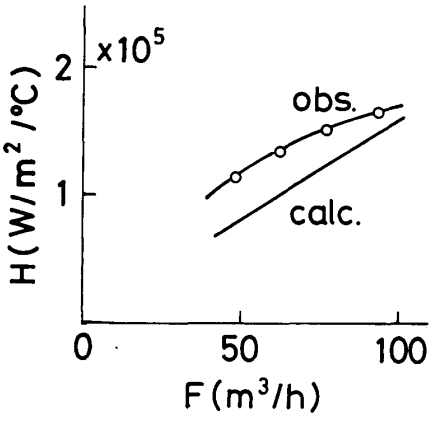

Fig. 9. Heat-transfer coefficient H vs flow rate F.

$$\delta T' = \frac{P}{4\pi\lambda t}\left[\frac{2b^2}{b^2 - h^2}\ln\frac{b}{h} - 1\right] , \qquad (9)$$

whwre λ is the thermal conductivity. It can be approximated for the Bitter disk that b is an half of the distance between the nearest holes and P is the total power in the disk divided by the number of holes. Numerical values are: h = 1.1 (mm), b = 3 $\sim$ 6 (mm), t = 0.6 (mm), λ = 3.8 (W/cm/°C), and P = 28 (W) for the 3-MW power of the coil, so $\delta T'$ = 13 $\sim$ 25 (°C) and the average temperature rise inside the conductor is estimated as $\overline{\delta T'} \approx 14$ (°C). The temperature difference between conductor and water, $T_\ell - T_0$ in Fig. 8, is equal to $\overline{\delta T'} + \delta T$, and we can obtain the heat-transfer coefficient H in eq.(7). The results for various values of F are summarized in Fig. 9.

Theoretically the heat-transfer coefficient for turbulent flow in a tube with the friction factor f is given by[8] $St \cdot Pr^{2/3} = f/8$, with Stanton number $St = H/c\mu v$ (c: specific heat) and Prandtl number $Pr = \eta c/k$ (k: thermal conductivity). It was already mentioned that f = 0.06, $\mu = 10^3$ (kg/m^3) and $\eta \approx 6 \times 10^{-4}$ (kg/m/s). Since $c = 4.2 \times 10^3$ (J/kg/°C) and k = 0.63 (W/m/°C), we obtain $H = 1.25 \times 10^4\ v = 1.6 \times 10^3\ F$, where H is in W/m^2/°C, v in m/s and F in m^3/h. The calculated values are also shown in Fig. 9, being somewhat smaller than those observed. This suggests that the cooling-surface area A is effectively larger than N(nS + S'). It is worth-while to mention that the equation for H in Montgomery's book[7] is only applicable to a smooth tube (where $f = 0.184\,Re^{-0.2}$, so $H \propto v^{0.8}$), giving about one-third of the above-mentioned values.

Magnetic fields (flux density), B_0, measured with a Hall probe at the center of the coil were strictly proportional to the current, I; the relation is expressed as B_0(T) = 1.31 I(kA), in fair agreement

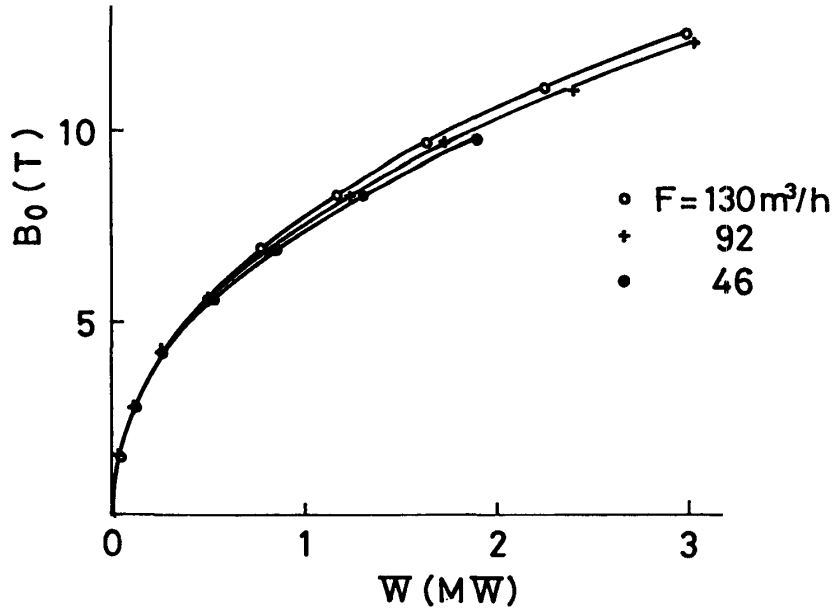

Fig. 10. Magnetic field (flux density) B_0 vs power W at flow rate F.

with that estimated in section II. If B_0 is plotted as a function of the power, the curves depend on the flow rate of water, as shown in Fig. 10. The field amounted to 12.4 T at 2.99 MW and 130 m^3/h. The uniformity of the field in the coil was also measured, the results being shown in Fig. 11. It is to be noted that the ratio of height to inner diameter of this coil is 3.78, being larger than the optimum value of 2.0[3] to produce the largest field with a given power.

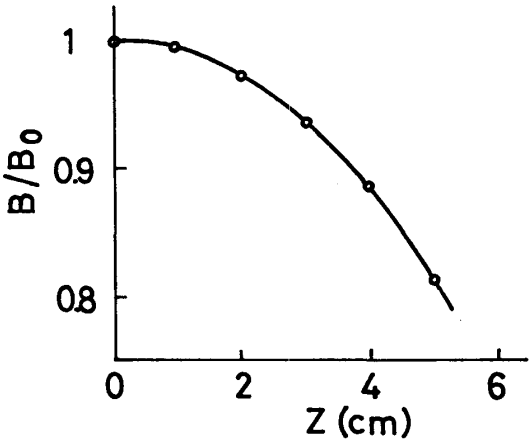

Fig. 11. Field distribution along the Z- axis of the Bitter coil.

V. Conclusions

The tests of the Bitter coil showed satisfactory results. The electric resistance and the water-flow resistance were in good agreement with those estimated. Also the magnetic field reached the expected value, while the temperature rise of the coil was rather smaller than the calculated value. If both 3.5-MW power and 150-m^3/h flow rate could be supplied, the field would easily exceed 13 T without dangerous heating of the coil. In order to utilize this coil for

a hybrid magnet, however, further considerations on the mechanical strength are indispensable. Full-hard copper or silver-copper alloys will be used to withstand the strong electromagnetic force exerted in the field of 20 T. Optimization calculations for the coil shape and current distribution, dealing with both thermal and mechanical limitations, have been reported elsewhere[9].

Acknowledgments

The authors express their hearty gratitude to Professor Y. Muto, Dr. K. Noto and Mr. K. Watanabe for their cooperation in the hybrid magnet project. They are indebted to Mr. H. Moriya for preparation of the manuscript. Thanks are also due to The Central Research Laboratory, Hitachi Ltd. for donating some equipments of the cooling system to augment the flow rate of deionized water. The work has been supported by Grant-in-Aid for Scientific Research (Grant No. 584009) of the Ministry of Education, Science and Culture.

References

(1) S. Maeda: High Magnetic Fields, Proc. Int. Conf., MIT, 1961 (Wiley, 1962) p. 406.

(2) T. Hirone: Les Champs Magnétique Intenses, Col. Int. CNRS, Grenoble, 1966 (CNRS, Paris, 1967) p. 107.

(3) F. Bitter: Sci. Instrum. 7 (1936) 482.

(4) N.F. Wood and D.B. Montgomery: Les Champs Magnétique Intenses, Col. Int. CNRS, Grenoble 1966 (CNRS, Paris, 1967) p. 91.

(5) P.A. Hudson and H. Jones: Cryogenics 20 (1980) 593.

(6) J.R. Clement: The Generation of High Magnetic Fields and their Application in Solid Physics, Lectures Int. Summer School, Würzburg, 1972, p. 136.

(7) D.B. Montgomery: Solenoid Magnet Design (Wiley-Interscience, New York, 1969).

(8) W.H. Giedt: Principles of Engineering Heat Transfer (Van Nostrand, New York, 1957).

(9) Y. Nakagawa: Proc. 7th Int. Conf. on Magnet Technology, Karlsruhe, 1981 (to be published in IEEE Trans. Mag.).